Composites: Part B 57 (2014) 112–119

Contents lists available at ScienceDirect

Composites: Part B

journal homepage: www.elsevier.com/locate/compositesb

Multi-line enhanced beam model for the analysis of laminated composite structures

Erasmo Carrera [a,b,*], Alfonso Pagani [a]

[a] Department of Mechanical and Aerospace Engineering, Politecnico di Torino, Corso Duca degli Abruzzi 24, 10129 Torino, Italy
[b] King Abdulaziz University, Jeddah, Saudi Arabia

ARTICLE INFO

Article history:
Received 3 September 2013
Accepted 23 September 2013
Available online 6 October 2013

Keywords:
A. Layered structures
B. Stress concentrations
C. Finite element analysis (FEA)
C. Laminate mechanics

ABSTRACT

A novel approach to the analysis of composite structure is introduced in this paper. One-dimensional (1D) refined finite elements are formulated by making use of the Carrera Unified Formulation (CUF). CUF is a higher-order 1D formulation which was recently introduced by the first author. By exploiting the hierarchical characteristics of CUF, a multi-line approach is developed straightforwardly and used for the analysis of multilayered structures. In the multi-line approach, each layer is modeled by one beam-line discretization. Refined beam elements with different orders of expansion over the cross-sectional plane are then employed along different beam-lines. The compatibility of displacements at the boundary interfaces between beam-lines is ensured by using Lagrange multipliers. The accuracy of the proposed method is verified both through published literature and through finite element solutions using the commercial code MSC/Nastran.

1. Introduction

This paper is devoted to the analysis of laminated composite beams. The advantages of composite materials are well known and the most relevant are: high strength-to-weight ratio, high stiffness-to-weight ratio, ease of formability, wide range of operating temperatures, and their capability to be tailored according to a given requirement (see the book by Tsai [1]). One of the main issues related to the proper modeling of a composite structure is related to its low transverse shear moduli compared to the axial tensile moduli, as discussed in the excellent review of Kapania and Raciti [2,3] which includes a comprehensive overview on composite beam works. Moreover, the characterization of anisotropic layered composite structures requires models able to reproduce piecewise continuous displacement and transverse stress fields in the thickness direction. These two effects, summarized as C_z^0 requirements in [4], are not automatically satisfied by those models that were originally devoted to the analysis of single-layered structures, such as the classical beam theories by Euler [5] (hereinafter referred to as EBBM) and Timoshenko [6] (hereinafter referred to as TBM).

A great deal of literature exists on classical and refined beam theories for the analysis of multilayered composite structures. A brief, though not exhaustive review, is given hereafter. Reddy [7] presented a plate theory which provides a parabolic distribution of the transverse shear strains ensuring that the transverse shear stresses are null on the top and bottom surfaces. By using this model, exact closed-form solutions for static analyses of cross-ply laminated beams with arbitrary boundary conditions were presented in [8]. In [9], Surana and Nguyen presented an interesting two-dimensional hierarchical curved beam element. In Matsunaga's paper [10], the displacement components were expanded into power series of the z-thickness coordinate. Mantari et al. [11] expressed the displacement components of laminated plates by adopting a combination of exponential and trigonometric functions. Recently, Vidal et al. [12] proposed the approximation of the displacement field as a sum of separated functions of axial and transverse coordinates by adopting the Proper Generalized Decomposition procedure.

All the aforementioned theories are based on the Equivalent Single layer (ESL) approach and, although the results agree very well with the three-dimensional solutions for several structural problems, the main drawback is the continuity of shear strains at interfaces (hence the discontinuity of the shear stresses if they are computed through the constitutive equations). To overcome this shortcoming, many researchers have adopted the Layer-wise (LW) approach and a few examples are given here. Shimpi and Ghugal [13] presents a new Layer-wise (LW) trigonometric model for two-layered cross-ply beams. The main feature of this theory is that the shear stresses are derived directly from the constitutive equations satisfying both the shear-stress-free condition at the free surfaces of the beam and the condition of continuity of the shear

* Corresponding author at: Department of Mechanical and Aerospace Engineering, Politecnico di Torino, Corso Duca degli Abruzzi 24, 10129 Torino, Italy.
E-mail addresses: erasmo.carrera@polito.it (E. Carrera), alfonso.pagani@polito.it (A. Pagani).

1359-8368/$ - see front matter © 2013 Elsevier Ltd. All rights reserved.
http://dx.doi.org/10.1016/j.compositesb.2013.09.046

stresses at the interface. On the same topic, Tahani [14] proposes two theories to analyze the static and dynamic behavior of the laminated beams. Unfortunately, when the number of layers increases, the LW approach becomes unfavorable because it is too expensive in terms of computational cost. To overcome this problem, many researchers have introduced layer independent theories in which zig-zag or Heaviside's functions are used.

Murakami [15] was the first to introduce a zig-zag function into Reissner's new mixed variational principle to develop a plate theory (for a comprehensive review of Murakami's zig-zag method, see Carrera [16]). Vidal and Polit [17] presented a refined sine model by exploiting a Heaviside function for each layer to satisfy the continuity conditions for both displacements and transverse shear stress and the free conditions of the upper and lower surfaces. An extensive investigation about the use of various cross-sectional functions for the analysis of laminated beams has recently been proposed in [18], where polynomial, trigonometric, exponential, as well as any combination of these functions were used.

It is clear that many attempts have been made in order to provide a general and reliable theory able to capture every aspect of the complex nature of composite materials. In the present paper, a new method for the analysis of laminated composite structures is proposed. This method, which is called *Multi-Line* (ML), represents a step forward from the classical ESL and LW approaches. ML models have recently been introduced by Carrera and Pagani [19] and used for the analysis of thin-walled and reinforced structures. In the present paper ML approach is extended to the analysis of composite structures. In a ML modeling approach for laminates, each layer (or group of layers) of the structure is modeled by one higher-order beam. Subsequently, higher-order beams are assembled at the layer interfaces through Lagrange multipliers. In this work, refined beam elements are formulated using the Carrera Unified Formulation (CUF). According to CUF, Taylor-like polynomials are used on the cross-section of each beam to expand generalized displacement variables in the neighborhood of the beam axis. CUF was originally devoted to the analysis of plate and shell structures [20] and recently it has been expanded to 1D theories by the first author and his co-workers [21]. Several papers are available on the analysis of composite structures via CUF models, see for example [18,22–24].

In the next sections a brief overview on CUF and the ML approach is provided. Numerical results concerning laminated and composite structures are then discussed. Finally, the main conclusions are outlined.

2. Higher-order beam formulation

2.1. Preliminaries

The adopted rectangular cartesian coordinate system is shown in Fig. 1, together with the geometry of a beam which can be considered as a single layer, a group of layers, as well as a whole multilayer. The cross-sectional plane of the structure is denoted by Ω, and the beam boundaries over y are $0 \leqslant y \leqslant l$. Subscript k, which is usually used to denote variables and parameters related to the kth layer, is neglected in the following for the sake of simplicity. Let us introduce the transposed displacement vector,

$$\mathbf{u}(x,y,z) = \{\, u_x \quad u_y \quad u_z \,\}^T \tag{1}$$

The stress, $\boldsymbol{\sigma}$, and strain, $\boldsymbol{\epsilon}$, components are grouped as follows:

$$\begin{aligned} \boldsymbol{\sigma}_p &= \{\, \sigma_{zz} \quad \sigma_{xx} \quad \sigma_{zx} \,\}^T, \quad \boldsymbol{\epsilon}_p = \{\, \epsilon_{zz} \quad \epsilon_{xx} \quad \epsilon_{zx} \,\}^T \\ \boldsymbol{\sigma}_n &= \{\, \sigma_{zy} \quad \sigma_{xy} \quad \sigma_{yy} \,\}^T, \quad \boldsymbol{\epsilon}_n = \{\, \epsilon_{zy} \quad \epsilon_{xy} \quad \epsilon_{yy} \,\}^T \end{aligned} \tag{2}$$

In the case of small displacements with respect to a characteristic dimension in the plane of Ω, the linear strain–displacement relations are used.

$$\begin{aligned} \boldsymbol{\epsilon}_p &= \mathbf{D}_p \mathbf{u} \\ \boldsymbol{\epsilon}_n &= \mathbf{D}_n \mathbf{u} = (\mathbf{D}_{n\Omega} + \mathbf{D}_{ny})\mathbf{u} \end{aligned} \tag{3}$$

where $\mathbf{D}_p$ and $\mathbf{D}_n$ are linear differential operators and the subscript "n" stands for terms lying on the cross-section, while "p" stands for terms lying on planes which are orthogonal to Ω.

$$\mathbf{D}_p = \begin{bmatrix} 0 & 0 & \frac{\partial}{\partial z} \\ \frac{\partial}{\partial x} & 0 & 0 \\ \frac{\partial}{\partial z} & 0 & \frac{\partial}{\partial x} \end{bmatrix}, \quad \mathbf{D}_{n\Omega} = \begin{bmatrix} 0 & \frac{\partial}{\partial z} & 0 \\ 0 & \frac{\partial}{\partial x} & 0 \\ 0 & 0 & 0 \end{bmatrix}, \quad \mathbf{D}_{ny} = \begin{bmatrix} 0 & 0 & \frac{\partial}{\partial y} \\ \frac{\partial}{\partial y} & 0 & 0 \\ 0 & \frac{\partial}{\partial y} & 0 \end{bmatrix} \tag{4}$$

Constitutive laws are now exploited to obtain stress components to give

$$\boldsymbol{\sigma} = \widetilde{\mathbf{C}}\boldsymbol{\epsilon} \tag{5}$$

Eq. (5) can be split into $\boldsymbol{\sigma}_p$ and $\boldsymbol{\sigma}_n$ with the help of Eq. (2) so that

$$\begin{aligned} \boldsymbol{\sigma}_p &= \widetilde{\mathbf{C}}_{pp}\boldsymbol{\epsilon}_p + \widetilde{\mathbf{C}}_{pn}\boldsymbol{\epsilon}_n \\ \boldsymbol{\sigma}_n &= \widetilde{\mathbf{C}}_{np}\boldsymbol{\epsilon}_p + \widetilde{\mathbf{C}}_{nn}\boldsymbol{\epsilon}_n \end{aligned} \tag{6}$$

The matrices $\widetilde{\mathbf{C}}_{pp}, \widetilde{\mathbf{C}}_{nn}, \widetilde{\mathbf{C}}_{pn}$, and $\widetilde{\mathbf{C}}_{np}$ contains the material coefficients. They can be found in [25] in the case of orthotropic material, which is considered in this work.

Within the framework of CUF, the displacement field $\mathbf{u}(x,y,z)$ can be expressed as

$$\mathbf{u}(x,y,z) = F_\tau(x,z)\mathbf{u}_\tau(y), \quad \tau = 1,2,\ldots,M \tag{7}$$

where F_τ are the functions of the coordinates x and z on the cross-section. $\mathbf{u}_\tau$ is the vector of the *generalized* displacements, M stands for the number of terms used in the expansion, and the repeated subscript, τ, indicates summation. The choice of F_τ determines the class of the 1D CUF model that is required and subsequently to be adopted. TE (Taylor expansion) 1D CUF models – described by Eq. (7) – consists of a Maclaurin series that uses the 2D polynomials $x^i z^j$ as base, where i and j are positive integers. For instance, the displacement field of the second-order ($N = 2$) TE model can be expressed as

$$\begin{aligned} u_x &= u_{x_1} + x\,u_{x_2} + z\,u_{x_3} + x^2\,u_{x_4} + xz\,u_{x_5} + z^2\,u_{x_6} \\ u_y &= u_{y_1} + x\,u_{y_2} + z\,u_{y_3} + x^2\,u_{y_4} + xz\,u_{y_5} + z^2\,u_{y_6} \\ u_z &= u_{z_1} + x\,u_{z_2} + z\,u_{z_3} + x^2\,u_{z_4} + xz\,u_{z_5} + z^2\,u_{z_6} \end{aligned} \tag{8}$$

The order N of the expansion is set as an input option of the analysis; the integer N is arbitrary and defines the order of the beam theory. The Timoshenko beam model (TBM) can be realized by using a suitable F_τ expansion. Two conditions have to be imposed: (1) a first-order ($N = 1$) approximation kinematic field and (2) the displacement components u_x and u_z have to be constant above the cross-section. By contrast, the Euler–Bernoulli beam model (EBBM) can be obtained through the penalization of ϵ_{xy} and ϵ_{zy}. Classical theories and first-order models ($N = 1$) require the necessary assumption of reduced material stiffness coefficients to correct Poisson's locking (see [26]). In this paper, Poisson's locking is corrected according to

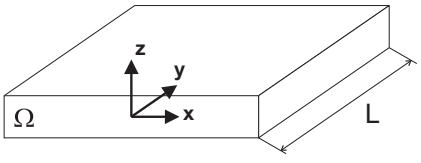

Fig. 1. Coordinate frame of the beam model.

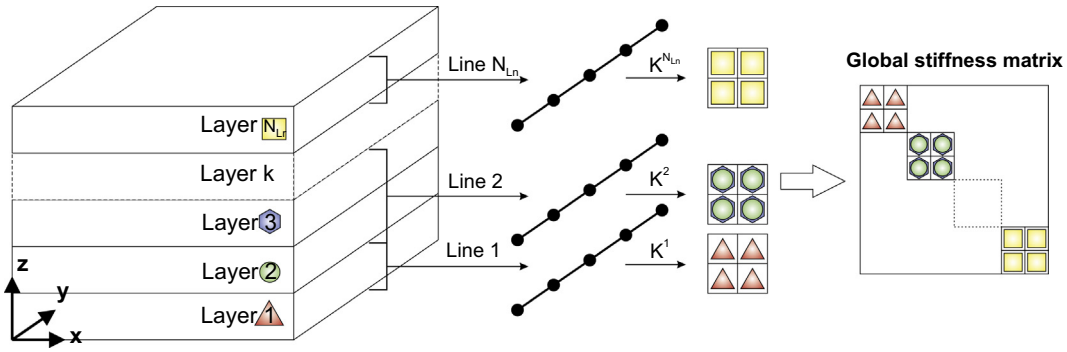

Fig. 2. Multilayered structures and Multi-Line approach.

the method outlined by Carrera et al. [21], where a detailed description of TE CUF models can be found.

2.2. Refined 1D finite elements

The finite element (FE) approach is used to discretize the structure along the y-axis. This process is conducted via a classical FE technique, where the displacement vector is given by

$$\mathbf{u}(x,y,z) = F_\tau(x,z)N_i(y)\mathbf{q}_{\tau i} \tag{9}$$

N_i stands for the shape functions and $\mathbf{q}_{\tau i}$ for the nodal displacement vector. For the sake of brevity, the shape functions are not reported here. They can be found in many books, for instance in [27]. Elements with four nodes (B4) are used in this work, that is, a cubic approximation along the y-axis is assumed. The choice of the theory order N is completely independent of the choice of the 1D FE to be used along the axis of the beam.

The principle of virtual displacements is used to derive the elemental stiffness matrix and the external loading vector.

$$\delta L_{\text{int}} = \int_V (\delta\boldsymbol{\epsilon}_p^T\boldsymbol{\sigma}_p + \delta\boldsymbol{\epsilon}_n^T\boldsymbol{\sigma}_n)\mathrm{d}V = \delta L_{\text{ext}} \tag{10}$$

where L_{int} stands for the strain energy and L_{ext} is the work done by the external loadings. δ stands for the usual virtual variation operator. The virtual variation of the strain energy is rewritten using Eqs. (3), (6) and (9).

$$\delta L_{\text{int}} = \delta\mathbf{q}_{\tau i}^T\boldsymbol{K}^{ij\tau s}\mathbf{q}_{sj} \tag{11}$$

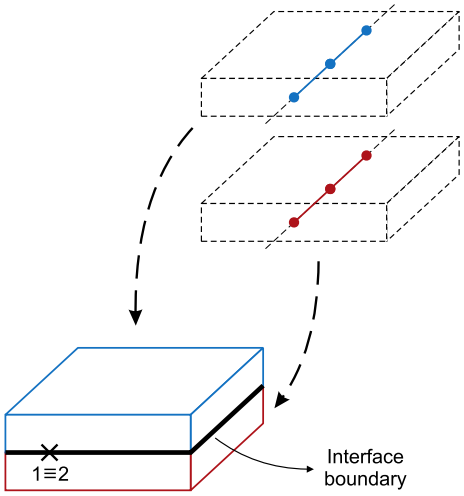

Fig. 3. Use of Lagrange multipliers to impose compatibility at boundary interface.

Table 1
Non-dimensional displacement at the tip, anti-symmetric laminated beam.

Model	u_z^*	DOFs
	Present ML	
ML3/3	42.30	1320
	MSC Nastran, [18]	
Solid	43.09	198,300
	Classical and higher-order ESL, [18]	
$N = 6$ with *ZZ*	42.26	1914
$N = 6$	42.16	1848
$N = 3$ with *ZZ*	41.66	726
$N = 3$	41.63	660
TBM	40.88	110
EBBM	31.96	66

$\boldsymbol{K}^{i\,j\tau s}$ is the stiffness matrix in the form of the fundamental nucleus. In a compact notation, it can be written as

$$\begin{aligned}\boldsymbol{K}^{ij\tau s} &= I_l^{ij} \triangleleft (\boldsymbol{D}_{np}^T F_\tau \boldsymbol{I})\left[\widetilde{\boldsymbol{C}}_{np}(\boldsymbol{D}_p F_s \boldsymbol{I}) + \widetilde{\boldsymbol{C}}_{nn}(\boldsymbol{D}_{np} F_s \boldsymbol{I})\right] \\ &+ (\boldsymbol{D}_p^T F_\tau \boldsymbol{I})\left[\widetilde{\boldsymbol{C}}_{pp}(\boldsymbol{D}_p F_s \boldsymbol{I}) + \widetilde{\boldsymbol{C}}_{pn}(\boldsymbol{D}_{np} F_s \boldsymbol{I})\right] \triangleright_\Omega \\ &+ I_l^{ij,y} \triangleleft \left[(\boldsymbol{D}_{np}^T F_\tau \boldsymbol{I})\widetilde{\boldsymbol{C}}_{nn} + (\boldsymbol{D}_p^T F_\tau \boldsymbol{I})\widetilde{\boldsymbol{C}}_{pn}\right] F_s \triangleright_\Omega \boldsymbol{I}_{\Omega y} \\ &+ I_l^{i,yj} \boldsymbol{I}_{\Omega y} \triangleleft F_\tau \left[\widetilde{\boldsymbol{C}}_{np}(\boldsymbol{D}_p F_s \boldsymbol{I}) + \widetilde{\boldsymbol{C}}_{nn}(\boldsymbol{D}_{np} F_s \boldsymbol{I})\right] \triangleright_\Omega \\ &+ I_l^{i,yj,y} \boldsymbol{I}_{\Omega y} \triangleleft F_\tau \widetilde{\boldsymbol{C}}_{nn} F_s \triangleright_\Omega \boldsymbol{I}_{\Omega y}\end{aligned} \tag{12}$$

where

$$\boldsymbol{I}_{\Omega y} = \begin{bmatrix} 0 & 1 & 0 \\ 1 & 0 & 0 \\ 0 & 0 & 1 \end{bmatrix} \triangleleft \cdots \triangleright_\Omega = \int_\Omega \cdots d\Omega \tag{13}$$

$$\left(I_l^{ij},\ I_l^{ij,y},\ I_l^{i,yj},\ I_l^{i,yj,y}\right) = \int_l \left(N_i\ N_j,\ N_i\ N_{j,y},\ N_{i,y}\ N_j,\ N_{i,y}\ N_{j,y}\right) dy \tag{14}$$

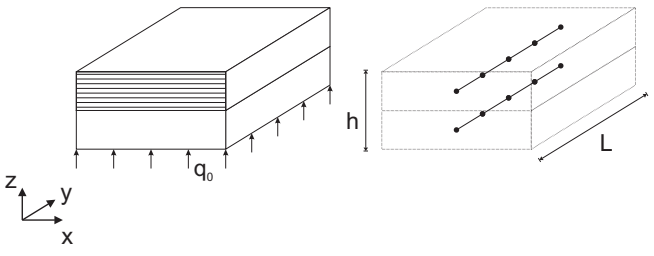

Fig. 4. ML approach to the analysis of the anti-symmetric laminated [0/90] beam.

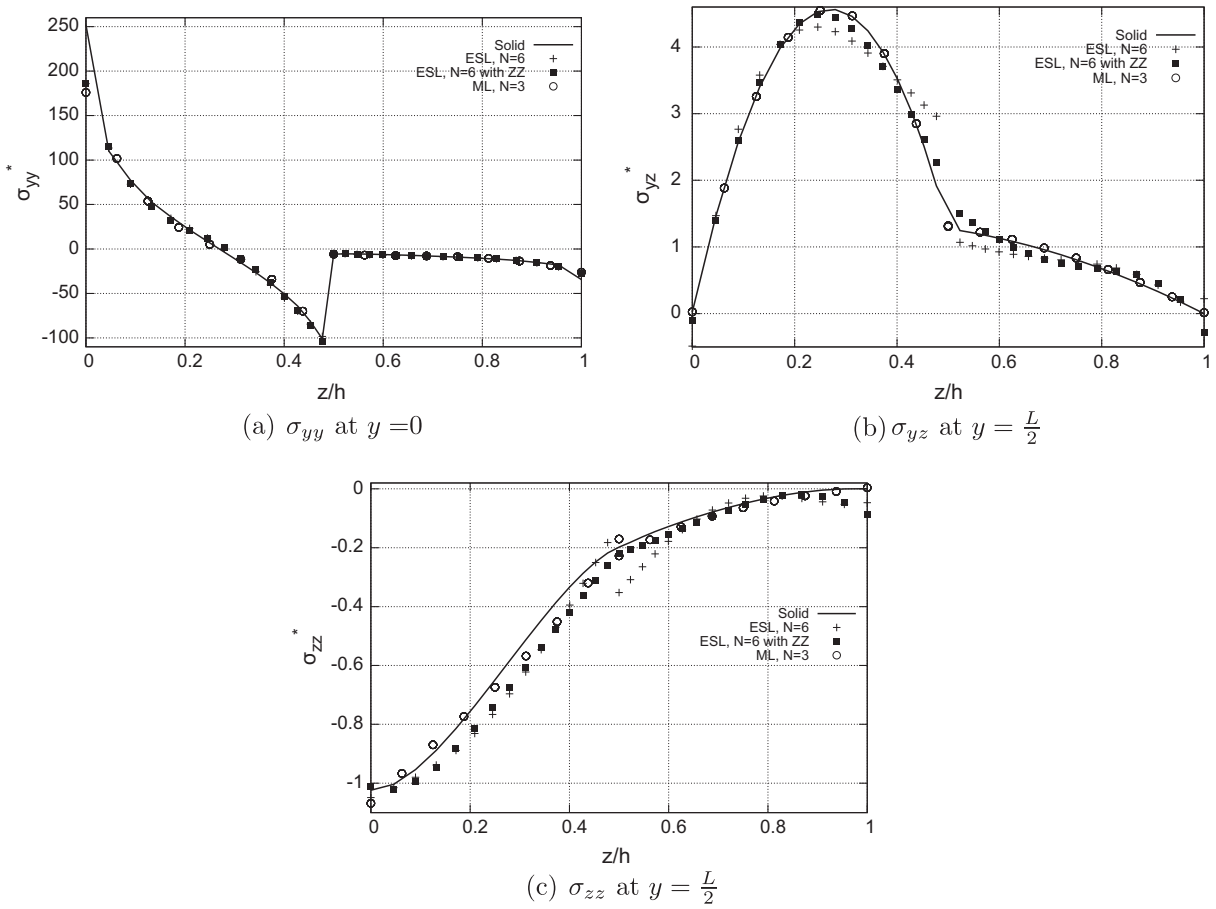

Fig. 5. Distribution of axial, σ^*_{yy}, and transverse, σ^*_{yz} and σ^*_{zz}, stresses for the anti-symmetric laminated beam.

It should be noted that $\mathbf{K}^{ij\tau s}$ does not depend either on the expansion order or on the choice of the F_τ expansion polynomials. These are the key-points of CUF which allows, with only nine FORTRAN statements, the implementation of any-order of multiple class theories.

For the sake of brevity, the derivation of the loading vector from the virtual variation of the work of external loadings, δL_{ext}, is not provided in this paper. It can be found in [21] for different loading conditions.

3. Multi-line refined beam models

The method of Lagrange multipliers provides the stationary conditions of a constrained functional. The application of Lagrange multipliers to CUF has recently been presented in [28], where Lagrange multipliers are used to implement higher-order 1D models with variable kinematic field along the beam axis. A more generic discussion of the Lagrange multipliers method can be found in [29,30], whereas Zienkiewicz and Taylor [31] show the use of multipliers in Finite Element Method (FEM) for contact and tied interfaces, for multibody coupling and to avoid the necessity of C^1 continuity for the problem of thin plates.

In the present paper, Lagrange multipliers are used to implement ML models for composite structures analysis. In Fig. 2 a multilayered structure is considered. The structure is composed by N_{Lr} layers. Each layer has its own geometrical and material properties. In the ML modeling approach, each layer (or group of layers) of the structure is modeled by a higher-order beam. Choice of the analyst is the number of beam lines N_{Ln} to be used in order to find the right balance between accuracy and efficiency. In the present paper, each beam line is discretized by means of refined CUF beam

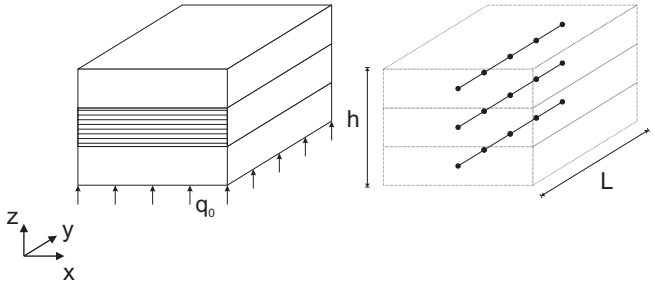

Fig. 6. Symmetric laminated [0/90/0] beam.

Table 2
Non-dimensional displacement at the tip and stress components, symmetric cross-ply beam. σ^*_{yy} at $(b,0,0.867h)$ and σ^*_{zz} at $(b,L/2,0)$.

Model	u^*_z	$-\sigma^*_{yy}$	$-\sigma^*_{zz}$	DOFs
		Present ML		
ML2/2/2	17.69	32.72	1.01	1188
ML3/2/3	17.83	25.69	1.03	1716
		MSC Nastran, [18]		
Solid	17.98	30.58	1.03	103,920
		Classical and higher-order ESL, [18]		
$N=6$ with ZZ	17.84	27.36	1.03	1914
$N=6$	17.14	25.29	0.99	1848
$N=3$ with ZZ	17.83	31.17	1.02	726
$N=3$	16.76	28.38	1.04	660
TBM	14.02	36.52	0.00	110
EBBM	6.22	36.52	0.00	66

elements, according to the previous section. Once the stiffness matrices of each beam line have been computed, the global stiffness matrix is assembled according to Fig. 2. Subsequently, compatibility constraints are imposed at a number of points at boundary interfaces ("connecting points") between beam lines. These conditions are imposed through Lagrange multipliers.

If we consider two points, 1 and 2, sharing the same position on the interface boundary (see Fig. 3), the *Lagrangian* that has to be added to the original problem in order to impose the equality of displacements is

$$\Pi = \boldsymbol{\lambda}^T(\mathbf{u}^1 - \mathbf{u}^2) \tag{15}$$

where $\mathbf{u}^1$ and $\mathbf{u}^2$ are the displacements of points 1 and 2, respectively. Points 1 and 2 belong to different beam-lines. $\boldsymbol{\lambda}$ is the vector containing the Lagrange multipliers. Eq. (15) is rewritten in terms of CUF with the help of Eq. (9).

$$\Pi = \boldsymbol{\lambda}^T \mathbf{B}\mathbf{q} \tag{16}$$

The explicit form of matrix $\mathbf{B}$ can be found in [28].

The solution of the problem is given by finding $\mathbf{q}$ and $\boldsymbol{\lambda}$ from the following linear system:

$$\begin{cases} \mathbf{K}\mathbf{q} + \dfrac{\partial \Pi}{\partial \mathbf{q}} = \mathbf{F} \\ \dfrac{\partial \Pi}{\partial \boldsymbol{\lambda}} = \overline{\mathbf{u}} \end{cases} \tag{17}$$

where $\mathbf{F}$ is the loadings vector and $\overline{\mathbf{u}}$ is equal to 0 for homogeneous conditions. Eq. (17) is rewritten using Eq. (16). In a matrix form it reads

$$\begin{bmatrix} \mathbf{K} & \mathbf{B}^T \\ \mathbf{B} & 0 \end{bmatrix} \begin{bmatrix} \mathbf{q} \\ \boldsymbol{\lambda} \end{bmatrix} = \begin{bmatrix} \mathbf{F} \\ 0 \end{bmatrix} \tag{18}$$

The use of the multipliers method offers many advantages. However, the main disadvantage of its use in structural problems is that the matrix of Eq. (18) is not, in general, positive definite.

4. Numerical results

In this section the accuracy and computational efficiency of the present higher-order ML models for the analysis of composite structures are demonstrated. First, analyses of cross-ply anti-symmetric and symmetric beams are discussed and the results are compared to classical and refined ESL models as well as to solid models from MSC/Nastran. Next, an eight-layer beam is considered and straightforward comparisons with some results from the literature are made. A sandwich tube is subsequently analyzed to highlight the capability of the present ML formulation to deal with LW solid solutions.

4.1. Anti-symmetric laminated beam

An anti-symmetric cross-ply [0°/90°], laminated beam is considered as the first assessment. The two laminae are assumed to be of the same thickness. The non-dimensional proprieties of the adopted orthotropic material are

$$E_L/E_T = 25 \quad G_{LT}/G_{TT} = 2.5 \quad \nu_{LT} = \nu_{TT} = 0.33$$

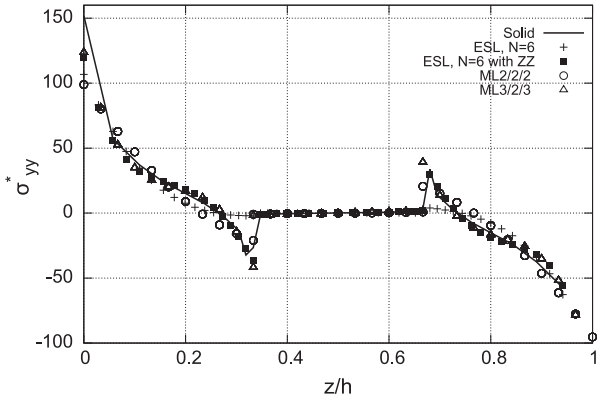

(a) σ_{yy} at $y = 0$

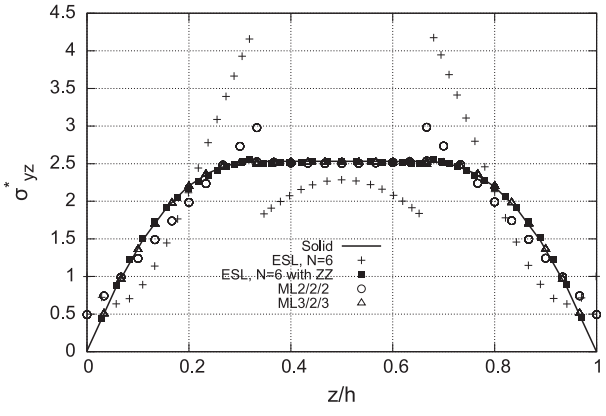

(b) σ_{yz} at $y = \frac{L}{2}$

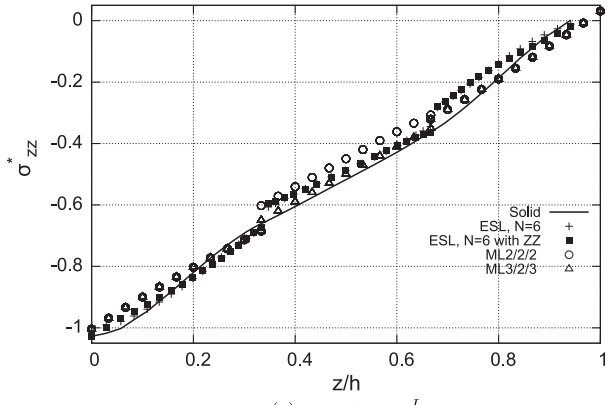

(c) σ_{zz} at $y = \frac{L}{2}$

Fig. 7. Distribution of axial, σ^*_{yy}, and transverse, σ^*_{yz} and σ^*_{zz}, stresses for the symmetric laminated beam.

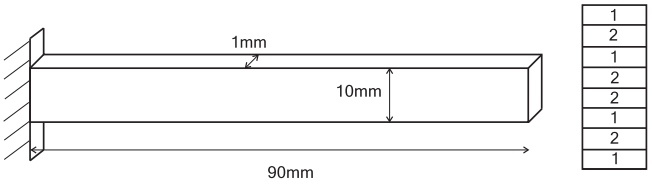

Fig. 8. 8-layer laminated beam.

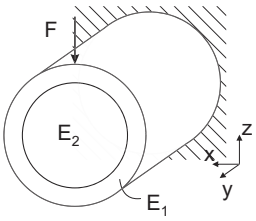

Fig. 10. Sandwich cylinder with soft core.

Table 3
Vertical displacement at the tip and normal stress at (0.5,45,5) mm, 8-layer laminated beam.

Model	$-u_z \times 10^2$ (mm)	$\sigma_{yy} \times 10^3$ (MPa)	DOFs
Present ML			
ML[3/3/3/2]$_s$	3.026	731	6696
Reference solutions			
Nguyen and Surana [9]	3.031	720	
Davalos et al. [32]	3.029	700	
Xiaoshan [33]	3.060	750	
Vo and Thai [34]	3.024		
Classical and higher-order ESL, [18]			
$N = 9$ with ZZ	3.040	661	5208
$N = 9$	3.039	661	5115
$N = 3$ with ZZ	3.040	729	1023
$N = 3$	3.039	729	930
TBM	2.988	730	155
EBBM	2.629	730	93

where L refers to the direction of the fibers and T stands for the direction normal to the fibers. For the sake of convenience, the results are given in non-dimensional form.

$$u_z^* = 100\frac{bh^3E_T}{q_0l^4}u_z, \quad \sigma_{ij}^* = \frac{\sigma_{ij}}{q_0}, \quad \text{with } i,j = x,y,z \tag{19}$$

here l is the length of the beam, whereas b and h are the dimensions of the rectangular cross-section. q_0 is the intensity of the load uniformly distributed over the lower face of the beam. The beam is considered to be very short ($l/h = 4$), with clamped-free boundary conditions.

Table 1 shows the displacement values at the tip for various models, including the solid FE model by the commercial code MSC/Nastran. The number of the degrees of freedom (DOFs) is also given in the last column for each model. In row 3, the results by the present ML model are given. The ML model is obtained by using two third-order ($N = 3$) beam-lines (see Fig. 4) and it is referred to as ML3/3 in the following. The results by the solid model and ESL beam models are taken from [18]. ESL denotes a one-line refined beam model and both classical and refined theories are considered in Table 1. In particular, refined beam models related to 6th and 3rd expansion orders above the cross-section are considered. For the refined ESL cases, the effect of the Zig-Zag (ZZ) Murakami functions was also investigated in [18] and the results are reported in Table 1. For all the beam models considered, seven 4-node (B4) beam elements are used in the FE discretization.

The results quoted clearly show the advantages of the ML approach over one-line beam solutions. The tip displacement obtained is, in fact, closer to solid solution. Furthermore it is obtained by using less DOFs than ESL cases, both with and without Zig-Zag functions.

The stress distributions over the beam cross-section in Fig. 5 (both normal and shear stress components are considered), confirm the superiority of ML analysis with respect to ESL cases.

4.2. Symmetric laminated beam

The analysis of a symmetric cross-ply [0°/90°/0°] laminated cantilever beam was carried out next. The beam is considered to be rectangular with width b and height h. The length-to-height ratio is $l/h = 4$. The three layers, which are made of the same material as in the previous case, have the same thickness. The ML scheme adopted is depicted in Fig. 6, together with the loading condition. The ML models addressed make use of three beam-lines. Two ML configurations are considered: (1) in the first case a second-order ($N = 2$) expansion is used in the three layers; and (2) in the second case a third-order ($N = 3$) expansion is used in the top/bottom layers, whereas a parabolic distribution on the cross-section is assumed in the central layer. ML models of the symmetric laminated beam are referred to as ML$\alpha/\beta/\gamma$, where α is the expansion order of the beam discretizing the bottom layer, β is the

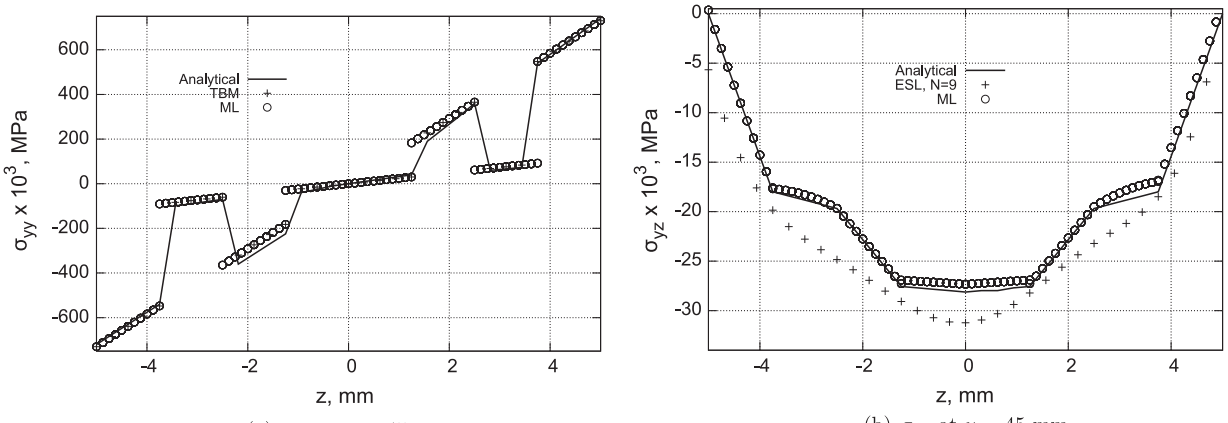

(a) σ_{yy} at $y = 45$ mm (b) σ_{yz} at $y = 45$ mm

Fig. 9. Distribution of axial, σ_{yy}, and transversal, σ_{yz}, stresses for the 8-layer laminated beam.

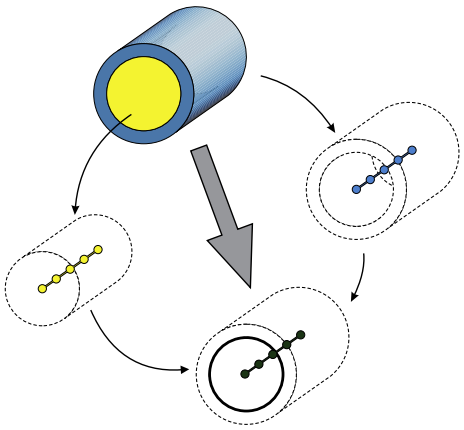

Fig. 11. From 3D problem to 1D multi-line model of sandwich cylinder.

Table 4
Vertical displacement at the tip and stresses, sandwich cylinder. σ_{yy} at $(0,0,R/2)$ and σ_{yz} at $(0,L/2,0)$.

	$-u_z \times 10^3$ (mm)	σ_{yy} (MPa)	$-\sigma_{yz}$ (MPa)	DOFs
		Present ML		
ML11/8	0.979	6.583	4.447	8976
		MSC Nastran		
Solid	0.982	6.667	4.465	24,060
		Classical and higher-order ESL		
$N = 10$	1.447	16.415	16.418	4356
$N = 8$	1.474	17.477	15.379	2970
$N = 6$	1.422	13.641	16.604	1848
$N = 4$	1.422	2.373	16.576	990
$N = 2$	1.231	2.398	8.165	396
TBM	1.300	2.296	7.543	110

expansion order of the central layer, and γ is the expansion order of the top layer.

The results are shown in Table 2, where the non-dimensional vertical displacement at the tip is given together with stress components. In particular, the values of σ^*_{yy} at $(b,0,0.867h)$ and σ^*_{zz} at $(b,L/2,0)$ are shown (the verification points are measured from the bottom left corner). The last column of Table 2 gives the number of the DOFs for each model considered. The results by ML models are compared to classical and refined ESL theories from [18] and to a solid FE model by MSC/Nastran. For both ML and ESL beam models, seven B4 elements were used along the beam axes.

ML analysis shows some convenience with respect to ESL, both with and without *ZZ*. However, such advantages are less evident than anti-symmetric laminate case. Stress distributions shown in Fig. 7 confirm this conclusion, even if it is evident from the figure that ESL models without through-the-thickness *ZZ* functions are not able to correctly detect transverse stress distributions. On the other hand, both ESL with *ZZ* and ML models are able to deal with solid-like analysis with very low computational costs.

4.3. Eight-layer composite beam

A cantilever beam composed by eight layers is considered as the third example. The geometric characteristics of the beam are shown in Fig. 8, together with the symmetric stacking sequence. The elastic modulus in the transversal direction (E_T), the shear moduli (G_{LT}, G_{TT}), and the Poisson's ratios (ν_{LT}, ν_{TT}) of the two orthotropic materials composing the laminae are equal and they are assumed to be 1 GPa, 0.5 GPa and 0.25 GPa, respectively. In contrast, the Young modulus along the fiber direction of the material labeled with the number 1 is 30 GPa whereas the one related to material 2 is 5 GPa. The structure is loaded at the free end with a concentrated load equal to $F_z = -0.2$ N.

In Table 3 the vertical displacement at the tip and the normal stress component at (0.5,45,5) mm are given (the coordinates of the verification point are measured from the bottom left corner). The ML model was implemented by using 8 beam-lines (i.e. one for each layer). Each beam line is discretized with ten B4 elements. The two central layers are modeled with a second-order ($N = 2$) beam theory in the ML model, whereas a third-order ($N = 3$) beam theory is used for the remaining six layers. For this reason, the ML model is referred to as ML$[3/3/3/2]_s$ in Table 3. The results by the present approach are compared with solutions from the literature ([9,32–34]) as well as with classical and refined ESL models from [18].

The LW capabilities of the present ML approach are clearly evident from the analysis of the 8-layer case as well as from the stress distributions in Fig. 9, where ML and ESL beam models are compared to the analytical solution derived by theory of elasticity presented in [35].

4.4. Sandwich cylinder with soft core

A sandwich cylinder is considered as the last example. The structure consists of an external ring and an internal core made of two different materials. The external ring is made of an aluminum alloy with elastic modulus $E_1 = 75$ GPa and Poisson ratio

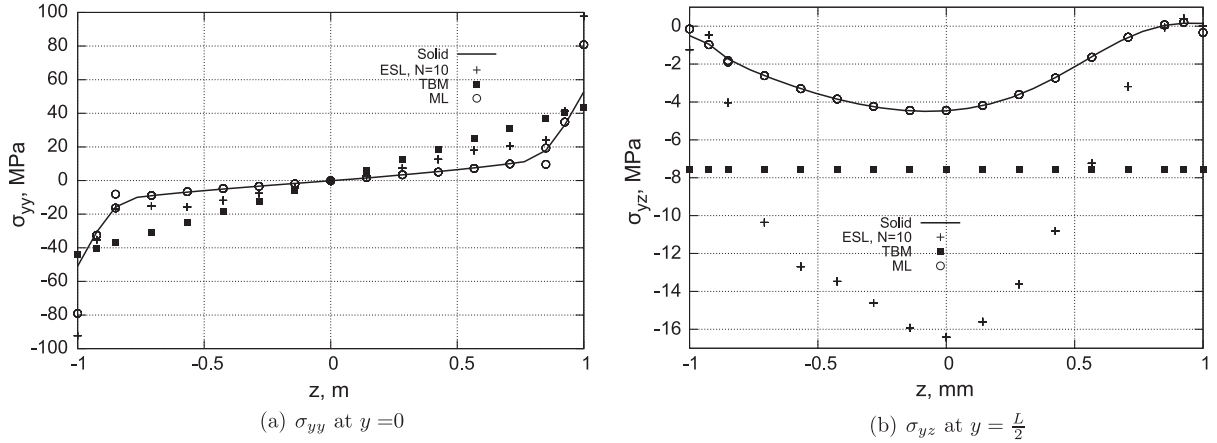

(a) σ_{yy} at $y = 0$ (b) σ_{yz} at $y = \frac{L}{2}$

Fig. 12. Distribution of axial, σ_{yy}, and transversal, σ_{yz}, stresses for the sandwich cylinder.

$\nu = 0.3$. The material composing the internal core is such that $E_2/E_1 = 0.5$ (see Fig. 10). The external radius of the cylinder is $R_e = 1$ m, whereas the thickness of the external ring is 0.2 m. The length of the tube is $l = 2R_e$. The tube has clamped-free boundary conditions and it undergoes a vertical point load $F_z = 10^4$ N at $y = l$.

The ML model of the sandwich cylinder is implemented by using one beam-line for the external ring and one beam-line for the internal core, as shown in Fig. 11. The two beam-lines are then superimposed to model the structure as a whole and compatibility conditions on displacements at the boundary interface between the external ring and the inner core are enforced through Lagrange multipliers. Seven B4 elements are used for each beam-line. An eleventh-order ($N = 11$) theory is used to model the external ring, whereas an eight-order ($N = 8$) model is used for the inner core.

The ML model of the sandwich cylinder is compared to classical and higher-order ESL beam models and to a solid FE model by MSC/Nastran. The results are given in Table 4 and Fig. 12. ML analysis shows some advantages in terms of accuracy with respect to ESL case. However, the ML model demands higher computational costs than ESL models.

5. Conclusions

In the present paper a Multi-line enhanced beam formulation has been introduced by using the Carrera Unified Formulation, which furnishes a reliable formulation to deal with higher-order beam models with no geometrical restrictions by considering the expansion order as an input of the analysis. Different-order beam elements have been formulated and subsequently used over different beam-lines discretizing various multilayered structures. Beam-lines have then been coupled by imposing the compatibility of displacements at a number of connecting points at the boundary interface using Lagrange multipliers. Although the efficiency of the present approach has proven to be problem dependent, Multi-line modeling undoubtedly represents a step forward in the analysis of laminated composite structures and it is able to deal with solid layer-wise solutions with a significant reduction of the computational costs.

References

[1] Tsai SW. Composites design, 4th ed. Dayton, Think Composites; 1988.
[2] Kapania K, Raciti S. Recent advances in analysis of laminated beams and plates, Part I: shear effects and buckling. AIAA J 1989;27(7):923–35.
[3] Kapania K, Raciti S. Recent advances in analysis of laminated beams and plates, Part II: vibrations and wave propagation. AIAA J 1989;27(7):935–46.
[4] Carrera E. A class of two dimensional theories for multilayered plates analysis. Atti Accademia delle Scienze di Torino Memorie Sci Fisiche 1995;19–20:49–87.
[5] Euler L. De curvis elasticis, Lausanne and Geneva: Bousquet, 1744 (English translation: Oldfather WA, Elvis CA, Brown DM. Leonhard Euler's elastic curves. Isis 1933;20:72–160).
[6] Timoshenko SP. On the corrections for shear of the differential equation for transverse vibrations of prismatic bars. Philos Mag 1922;41:744–6.
[7] Reddy JR. A simple higher-order theory for laminated composites. J Appl Mech 1984;51:745–52.
[8] Reddy JR, Khdeir AA. An exact solution for the bending of thin and thick cross-ply laminated beams. Compos Struct 1997;37:195–203.
[9] Nguyen SH, Surana KS. Two-dimensional curved beam element with higher-order hierarchical transverse approximation for laminated composites. Comput Struct 1990;36:499–511.
[10] Matsunaga H. Interlaminar stress analysis of laminated composite beams according to global higher-order deformation theories. Compos Struct 2002;55:105–14.
[11] Mantari JL, Oktem AS, Guedes Soares C. A new higher order shear deformation theory for sandwich and composite laminated plates. Compos Part B: Eng 2012;43(3):1489–99.
[12] Vidal P, Gallimard L, Polit O. Composite beam finite element based on the proper generalized decomposition. Comput Struct 2012;102–103:76–86.
[13] Shimpi RP, Ghugal YM. A new layerwise trigonometric shear deformation theory for twolayered crossply beams. Compos Sci Technol 2001;61(9):1271–83.
[14] Tahani M. Analysis of laminated composite beams using layerwise displacement theories. Compos Struct 2007;79(4):535–47.
[15] Murakami H. Laminated composite theory with improved in-plane responses. J Appl Mech 1986;53(3):661–6.
[16] Carrera E. Historical review of zig-zag theories for multilayered plates and shells. Appl Mech Rev 2003;56(3):287–309.
[17] Vidal P, Polit O. A family of sinus finite elements for the analysis of rectangular laminated beams. Compos Struct 2008;84(1):56–72.
[18] Carrera E, Filippi M, Zappino E. Laminated beam analysis by polynomial, trigonometric, exponential and zig-zag theories. Eur J Mech A/Solids 2013;41:58–69. http://dx.doi.org/10.1016/j.euromechsol.2013.02.006.
[19] Carrera E, Pagani A. Analysis of reinforced and thin-walled structures by multi-line refined 1D/beam models. Int J Mech Sci 2013;75:278–287.
[20] Carrera E. Theories and finite elements for multilayered, anisotropic, composite plates and shells. Arch Comput Methods Eng 2002;9(2):87–140.
[21] Carrera E, Giunta G, Petrolo M. Beam structures: classical and advanced theories. John Wiley & Sons; 2011. http://dx.doi.org/10.1002/9781119978565.
[22] Carrera E. Theories and finite elements for multilayered plates and shells: a unified compact formulation with numerical assessment and benchmarking. Arch Comput Methods Eng 2003;10(3):216–96.
[23] Carrera E, Maiarú M, Petrolo M. Component-wise analysis of laminated anisotropic composites. Int J Solids Struct 2012;49:1839–51. http://dx.doi.org/10.1016/j.ijsolstr.2012.03.02.
[24] Carrera E, Petrolo M. Refined one-dimensional formulations for laminated structure analysis. AIAA J 2012;50(1):176–89. http://dx.doi.org/10.2514/1.J05121.
[25] Reddy JN. Mechanics of laminated composite plates and shells. Theory and analysis. 2nd ed. CRC Press; 2004.
[26] Carrera E, Brischetto S. Analysis of thickness locking in classical, refined and mixed multilayered plate theories. Compos Struct 2008;82(4):549–62.
[27] Bathe KJ. Finite element procedure. Prentice hall; 1996.
[28] Carrera E, Pagani A, Petrolo M. Use of Lagrange multipliers to combine 1D variable kinematic finite elements. Comput Struct, in press. http://dx.doi.org/10.1016/j.compstruc.2013.07.005.
[29] Courant R. Differential and integral calculus. Interscience Publishers; 1937.
[30] Strang G. Calculus. Welles-Cambridge Press; 1991.
[31] Zienkiewicz OC, Taylor RL. The finite element method for solid and structural mechanics. 6th ed. Washington: Butterworth Heinemann; 2005.
[32] Davalos JF, Kim Y, Barbero EJ. Analysis of laminated beams with a layerwise constant shear theory. Compos Struct 1994;28:241–53.
[33] Xiaoshan Lin YZ. A novel one-dimensional two-node shear-flexible layered composite beam element. Finite Elem Anal Des 2011;47:676–82.
[34] Vo TP, Thai HT. Static behavior of composite beams using various refined shear deformation theories. Compos Struct 2012;94:2513–22.
[35] Lekhnitskii SG. In: Tsai SW, Cheron T, editors. Anisotropic Plates. Gordon & Branch; 1968 (Translated from 2nd Russian Edition).